FABRICATION OF HIGH FREQUENCY SURFACE ACOUSTIC WAVE (SAW) DEVICES FOR REAL TIME DETECTION OF HIGHLY TOXIC CHEMICAL VAPORS

Upendra Mittal[2♦], Tarikul Islam[1*], A T Nimal[2], M U Sharma[2]

1. Department of Electrical Engineering, F/O Engineering & Technology, Jamia Millia Islamia (University), Jamia Nagar, New Delhi – 110025, India,

2. Solid State Physics Laboratory, Timarpur, Delhi-110054, India

♦PhD Research scholar, Department of Electrical Engineering, F/O Engineering & Technology, Jamia Millia Islamia, (University)

*corresponding author

Emails: Upendra.mittal@sspl.drdo.in, tislam@jmi.ac.in

Submitted: May 5, 2015 *Accepted: July 12, 2015* *Published: Sep. 1, 2015*

Abstract- In this paper, a low cost fabrication of sub micron features size SAW device with conventional lithography and their application for toxic chemical vapor detection has been presented. The SAW devices with different interdigital transducer (IDT) electrodes line widths were designed and fabricated. The fabricated SAW devices features had an accuracy of ± 0.1 µm. Frequency response of the SAW devices was measured with vector network analyzer for design parameter confirmation. The fabricated devices have been configured in multisensory oscillator configuration and tested with chemical ware fare agents simulants at very low concentration (ppb).

Index terms: SAW device, Optical lithography, RF characterization, Mass Loading, Chemical sensor

I. INTRODUCTION

Surface acoustic wave devices have been in industrial use for more than 60 years [1, 2]. The telecommunications industry is the major user of SAW devices, consuming approximately three billion devices annually, mainly in mobile cell phones and base stations [2]. There are several new emerging applications for surface acoustic wave devices as sensors that may eventually equal the demand of the telecommunications market. These include automotive applications (torque and tire pressure sensors), medical applications (biosensors), and industrial and commercial applications [3]. Surface acoustic wave (SAW) sensors are competitively priced, intrinsically rugged, highly responsive, intrinsically reliable and also capable of being passively and wirelessly interrogated (no sensor power source required) [2, 3].

In recent times, the applications of surface acoustic wave (SAW) devices have been extensively used for toxic chemical vapour sensing by exploiting the extreme sensitivity of SAW device to surface perturbation [5]. SAW devices can be used to monitor/sense gases and organic solvents, if these are coated with a material which selectively adsorbs molecules from air (Wohltjen 1984, Nisuveshuizess and Venema 1991, Fischeraner 1995, Avremov et al 2000).

Commonly used piezoelectric materials in classical SAW applications are ST-cut quartz and lithium niobate. Besides them ZnO, AlGaN, GaN, AlN are used [Zaki et al., 2006; Rufer et al., 2006; Assouar et al., 2000; Rufer et al., 2005; Kirsch et al., 2006; Kirsch et al., 2007; Omori et al., 2008]. Recently, multilayered substrates are used for the wave velocity increase [Ahmadi et al., 2004]. The highest velocities are achieved when the piezoelectric material is placed on the top of the diamond layer, due to its highest acoustic wave velocity [Assouar et al., 2000; Benetti et al. 2004; Benetti et al., 2005; Besmaine et al., 2008; Hakiki et al., 2005; Mortet et al., 2008; Jian et al., 2008; Shikata et al., 2005]. Several piezoelectric materials in combination with diamond/silicon substrates have been investigated theoretically and experimentally. Theoretical calculation of the wave velocity in the multilayer structures is based on the solution of the wave equation demanding elaborate numerical computations. The use of diamond in the multilayered SAW structure has the following advantages: high frequencies up to 5 GHz, high coupling coefficients up to 1.2%, small temperature deviations, high power capability, and small device size without submicron lithography [6]. The disadvantages of the layered SAW structures are the complex design and the problem

related to the deposition of a piezoelectric layer with appropriate crystalline orientation. These facts probably have caused insufficient research on SAW sensors using diamond. Keeping all these prior work complexity in mind, in present work SAWs are generated on classical piezoelectric material (ex. Quartz, and lithium niobate,) from electric signal interrogations.

SAW device have a pair of transmitting and receiving interdigital transducers (IDT), which consist of a long chain of electrodes separated by gaps. Minor defect during fabrication in these kinds of features can lead to the failure of the device. Hence for fabrication of SAW require high quality of fabrication process. Therefore SAW devices are made using photolithography, for precise control over the minimum feature size of the electrode geometry of a SAW device. This is one reason for the success of the SAW technology, another being that the crystal substrates have reproducible properties, so that SAW devices with very predictable performance can be produced. Photolithography is limited by the wavelength of the light used to reproduce the pattern on the substrate. Ultra-violet (UV) photolithography is one of the well adapted micro fabrication techniques to pattern micrometer sized features on substrates and realize micro-electro-mechanical-system (MEMS) devices [4].

The IDTs of SAW device is made of closely packed micro meter sized metal electrodes fabricated over piezoelectric substrates [3, 7]. The width of the electrode and gap length between the electrodes decides propagating SAW wavelength (λ) [2, 3]. The resonance frequency, f_0, of the SAW device is related to λ as

$$f_0 = V/\lambda \quad (1)$$

Where, V is the SAW velocity of the substrate. Thus, it is highly important to fabricate IDTs of required feature size to meet the performance of operation such as an anticipated frequency response [3]. Further, it is very crucial to fabricate patterns of required feature size without any anomalies such as short or open interconnects in the SAW IDT electrodes. UV lithography and electron beam lithography techniques are widely adopted techniques for fabricating SAW devise [2, 6, and 7].

Recent advancements in clean room technologies have enabled electronic device manufacturing industries to fabricate nanometre sized features [4, 7] with utmost accuracy, but initial capital investment as well as maintenance of this setup is very costly. Efforts have

also been made to fabricate SAW devices using newer fabrication techniques: for example Lai et al. [8] has proposed the near field phase shift photolithography (NFPSL) technique to fabricate submicron features and demonstrated the fabrication procedure for a 2.3 GHz surface acoustic wave (SAW) device with NFPSL technique [8]. Also, Forsén et al. [9] employed jet and flash nano imprint lithography to fabricate SAW sensors suitable for wireless temperature measurement and UV–LED lithography is also been used for microstructure patterning [10] but none of the technology is commercially available for SAW device fabrication. In present scenario where cost became major consideration the UV based contact lithography techniques is being proved to be the relatively simple and most cost effective techniques for SAW device fabrication. In the present work the SAW devices is fabricated at different frequency to verify the consistency of the fabrication process, different SAW device designs at different operating frequency were considered for the fabrication. Using the UV based contact lithography technique, SAW devices are processed for single and multisensory system for toxic chemical vapor detection at low concentration (ppb).

II. THEORY OF SAW BASED SENSORS

SAW devices can be used as sensors by using them in suitable configuration. In a SAW device since the acoustic energy is confined to the surface of few wavelengths thickness, hence any perturbations near the surface such as mechanical, electrical, temperature etc can be detected [3]. An acoustic device is thus sensitive mainly to physical parameters which may interact with (perturb) mechanical properties of the wave and its associated electrical field. In general, the surface acoustic phase velocity can be affected by many factors, each of which possesses a potential sensor response. Equation 2 illustrates the perturbation of the acoustic velocity by the mass (*mass*), electrical (*elec*), mechanical (*mech*) and environmental (*envir*) parameter properties. A sensor response may be due to a combination of these parameters [3].

$$\frac{\Delta V}{V_{acoustic}} \cong \frac{1}{V_{acoustic}}\left(\frac{\partial V}{\partial_{mass}}\Delta mass + \frac{\partial V}{\partial_{elec}}\Delta elec + \frac{\partial V}{\partial_{mech}}\Delta mech + \frac{\partial V}{\partial_{env}}\Delta env\right) \quad (2)$$

A SAW is an elastic wave that propagates confined to the surface of a semi-infinite medium, and its penetration depth being a fraction of its wavelength(λ). The interaction with any medium in contact with the SAW device surface affects frequency of the wave itself.

For SAW chemical sensors some transductions layers (i.e. polymer) is used to convert the value of the desired parameter (chemical agent concentration, etc) into a mechanical or electrical perturbation that can disturb the SAW properties. Since SAW devices convert electrical signals to mechanical waves and vice versa hence we make the SAW device a frequency selective element by configuring the SAW device in an oscillator configuration. For a SAW sensor coated with polymer, mass-loading mechanisms contribute to its response as shown in eq. (3).

$$\frac{\Delta f}{f_0} = -C_m f_0 \, \Delta \left(\frac{m}{A}\right) \tag{3}$$

in which c_m is the coefficients of mass sensitivity, (m/A) is the change in mass per unit area and f_0 is the fundamental frequency of the SAW device. From eq. 4 it is evident that if fundamental frequency of the SAW device increases the sensitivity of the sensor increases because it is directly proportional to square of the fundamental frequency of the SAW device [12, 13]

$$\Delta f / \Delta m \propto f_0^2 \tag{4}$$

Hence for the current work high frequency SAW devices (70 MHz to 500MHz) have been design and fabricated details are shown in Table 1.

Table 1: SAW device design details

Frequency (MHz)	Wavelength (µm)	Electrode Width/Gap (µm)	No of finger	Size (mm x mm)	Substrate	SAW velocity (m\s)
70	45.05	11.26	50	20x15	ST-X Quartz	3154
100	31.54	7.886	22	15x10	ST-X Quartz	3154
150	21.02	5.256	44	5x15	ST-X Quartz	3154
273	12.78	3.14	8	5x12	Y-Z Lithium Niobate	3488
500	6.976	1.57	5	5x5	ST-X Quartz	3154

III. DESIGN PARAMETER OF SAW DEVICE FOR SENSOR APPLICATION

While designing SAW devices for chemical sensors certain aspects such as type of the device, insertion loss, bandwidth, positioning of the devices in case of dual device, etc have to be taken care of [12-14]. Resonators and delay lines are the most commonly used devices for chemical sensor applications. Delay lines are comparatively less complex to design and pose less fabrication related criticalities than resonators, while the latter are advantageous where insertion loss is important. Sufficient space should be given between the IDTs for depositing chemical interface layer.

The basic parameters determining the performance of SAW device are wavelength (decided by IDTs), velocity (decided by substrate), amplitude and delay. To model the frequency response characteristics of SAW device on a piezoelectric substrate, two interrelated factors have been taken in to consideration [11, 14-17] (i) the geometry of thin film metallic inter-digital transducer (IDT) and (ii) the piezoelectric substrate. The IDT consists of a series of interleaved electrodes made from a metal film deposited on a piezoelectric substrate. The width of the electrodes is equal to the width of the electrode gaps. An applied voltage will cause (through piezoelectric effect) a strain of periodicity L, the periodicity of the structure. If the frequency is such that L is close to the wavelength (λ) of surface acoustic wave then there is a strong coupling into surface wave energy and surface waves are launched along the substrate.

To understand the behaviour of IDT, crossed-field equivalent circuit model is considered in which an IDT is represented by a three-port network as shown in fig.1. In this model, ports 1 and 2 represent electrical equivalents of “acoustic” ports while port 3 is considered as a true electrical port [16].

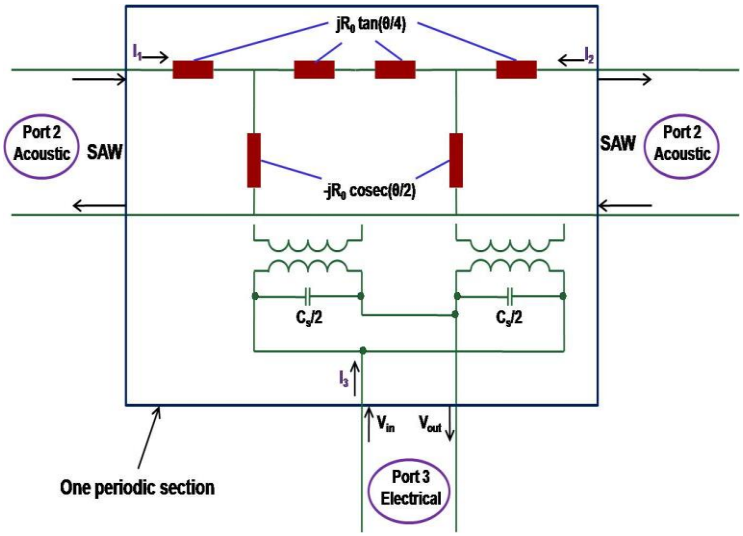

Figure 1. Cross-field equivalent circuit model

The electrical equivalents in ports 1 and 2 are those for an acoustic and passive SAW transmission line, while at port 3 actual signal voltages are applied or detected. The transducer is assumed to have N sections, each of length L, so that the total number of electrodes is 2N+1 (N input, N output and one electrical). Each section by analogy is assigned an equivalent circuit in which the electromechanical coupling constant will have a value appropriate for surface waves. The electrical circuit of the whole transducer is formed by cascading the circuits of individual sections, and gives the relationships between signals at the three ports. This three port model is used in SAW device simulation work.

IV. SIMULATION AND DESIGN

One side polished Y Cut X propagating lithium niobate and ST-X quartz wafers were chosen as substrate materials to fabricate devices as mentioned in Table I. ST-X quartz substrate is widely used for SAW sensor applications because of its zero first order Temperature Coefficient of Delay (TCD) at room temperature and lithium niobate has higher electromechanical coupling (K^2) hence are chosen as a substrate for the present work [17, 21]. The SAW device parameters (centre frequency, insertion loss, delay time and bandwidth) are determined by the electrode width and gap, number of electrode pairs in each IDT, aperture of the IDT and the distance between the centres of the two IDTs [22-26]. For achieving required output from design equivalent circuit model is used. The algorithms are implemented in Matlab for the three port equivalent circuit model of an IDT. As the responses for various parameters are large in number, to plot and compare them is a tedious

job. Hence VBA (Visual Basic for applications) macros are written in MS excel. The macros are (1) to open txt model file, (2) to kill spike at centre frequency (spikes are typical of this model since at centre frequency the value becomes infinity and needs to be omitted), (3) to name the sheets and move it to a single workbook and (4) to combine all the charts together. The four macros need to be run one after the other in the above sequence with their given shortcuts.

The effect of various parameters such as (i) velocity of SAW, (ii) coupling coefficient (k^2) of quartz substrate, (iii) width and gap of the electrodes of IDT, (iv) number of electrodes (finger pairs) of each IDT and (v) aperture are studied with this model. While the parameters (i) and (ii) above are materials (quartz and lithium niobate substrate) related parameters, the rest are the IDT's geometrical parameters. Though the material property is known, it is noted that these values vary slightly due to variation in material fabrication [22]. Thus it is advisable to incorporate such variations in the model itself, for taking care of unexpected change in SAW response. The geometrical properties are varied over a wide range to analyze the pattern of variation and to select the best combination for design. Finally considering various trades-offs a SAW devices were designed and fabricated as per details given in Table I. A delay of 1-2μs is incorporated in the entire devices so that sufficient gap is provided between the two IDTs for coating the selective and sensitive chemical adsorbent material for sensing applications.

The device structure was created using custom-made software "SAW Device Designer" written in Visual Basic. A snapshot of the software is shown in fig. 2.

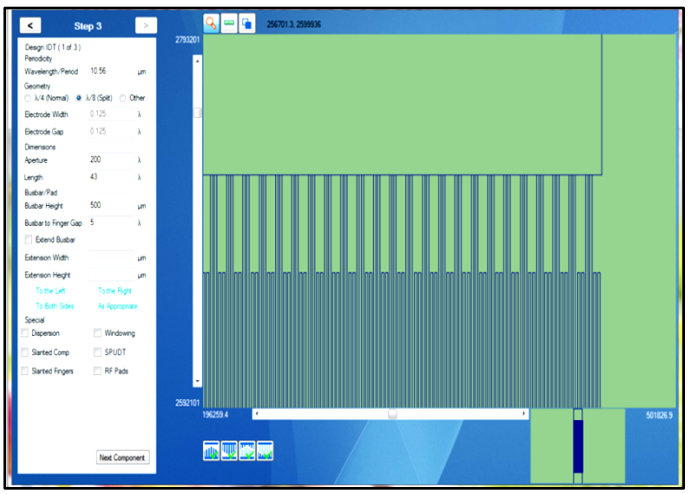

Figure 2. Screen shot of SAW device designer software

In addition to the above mentioned parameters, many parameters related to structural design and mask fabrication are fed in to the software. With this software, the IDT structures have been designed and saved in Data Exchange Format (DXF). Multiple devices are then arranged in a matrix for mask fabrication. Additional lines for aligning the dicing blade and the SAW direction on the quartz substrate are provided in the mask design. The devices are grouped in such a way that multiple devices (2 to 5) can be diced together for proper cancellation of spurious. While two devices are good enough to realize a chemical sensor which has one reference and one sensor device while five devices option is an added feature so that the same can be extended for use in electronic nose (multiple sensor) kind of system.

V. EXPERIMENTAL WORK

a. MASK FABRICATION

The mask design is made for a positive mask where the fabrication of the device will be carried out by photolithographic etching method.

The mask was fabricated using the data prepared in AUTOCAD and GDSII. It was verified and fed into a LASER Pattern generator after conversion. A resist (AZ1518) coated pre baked master grade chrome blank of size 4”X4” was loaded into the LASER pattern generator (Heidelbrg DWL 200). The mask was exposed using the data. After exposure, the mask plate was developed using MIF 300 developer. The pattern was inspected and subsequently, it was etched using chrome etchant. The mask was inspected and dimensions were measured and the remaining resist was removed using stripping solution. Finally, the mask was inspected for quality under microscope. This was then used for fabrication of SAW devices. The final mask images are presented in Fig 3 (a) and 2 (b). The critical dimension for these mask were 1.57, 3.14, 5.256, 7.886 and 11.26 µm.

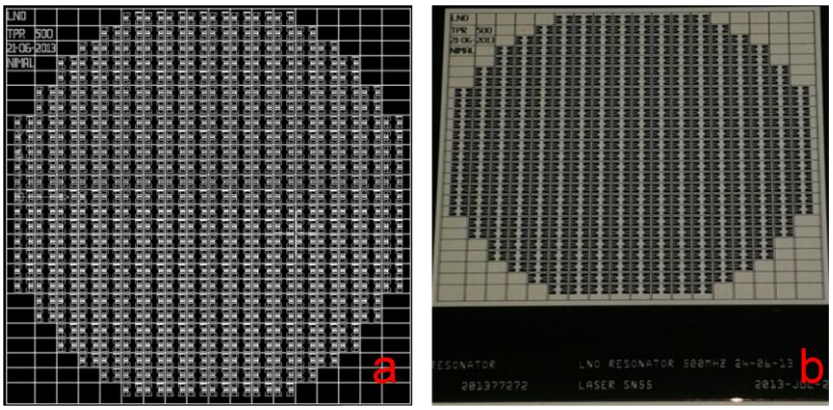

Figure 3. Fabricated mask images of 500 MHz SAW device (a) Designed (b) Fabricated

b. FABRICATION OF SAW DEVICE

Standard photolithography (PLG) technique was utilized for device fabrication; device processing flow diagram is shown in figure 4.

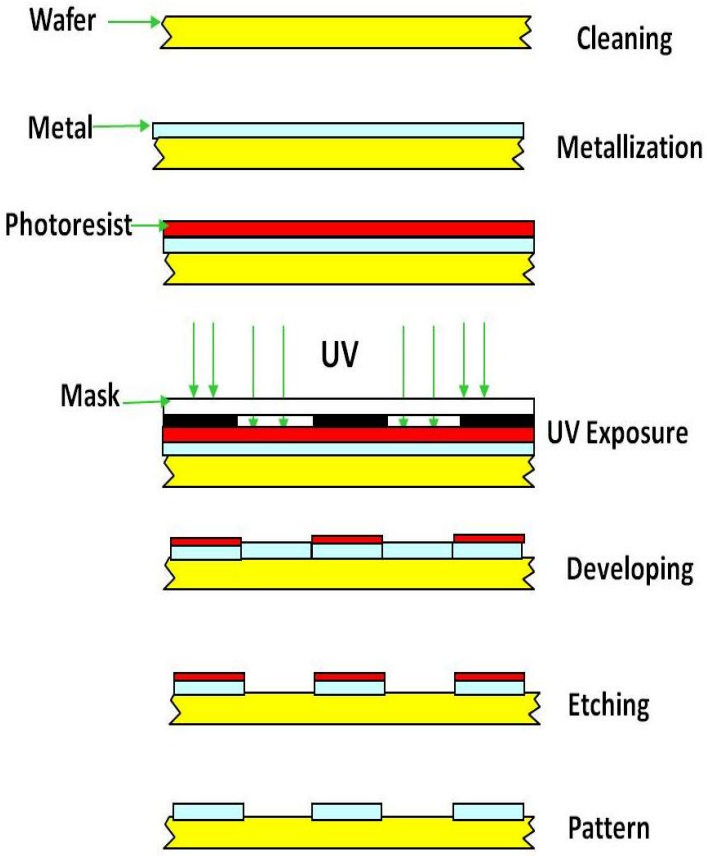

Figure 4. Photolithography flow chart for SAW device fabrication.

High purity aluminium (99.999) has been used for metallization. Aluminium metal was deposited on bare 3" quartz substrate using thermal evaporation system (model 12L). The coating thickness was controlled to 2000 Å by a thickness monitor. The substrate was then coated with AZ1505 positive photo-resist (supplied by microchem) using spin coater system. The samples were spun at rate of 4000 rpm for 30 s in order to achieve the thickness of 1 µm. The photo resist thickness is measured by ellipsometry system. The coated substrate was pre-baked at 90°C for about 30 min to dry solvents and enhance adhesion. The substrate was then exposed to UV rays (I line at 386 nm) for 8 sec under UV source of radiance 5500– 5800 JW/cm^2 through photo-mask using mask aligner (MJB3, Karl Suss). The exposed photo-resist was then developed using MIF 726 developer, then the samples were rinsed in DI (De Ionised) water to stop over development and dried using compressed clean air and examined under microscope for critical dimension measurement. After microscopic inspection post baking of the developed substrate was carried out at 120°C to dry the sample for about 60 sec and substrate is again examined under microscope. The exposed aluminium in between the photo-resist was then etched by an chemical etching process. Finally the photo-resist was stripped by acetone solution to remove the photo resist. The devices were then diced out of the wafer in set of two (for dual device configuration) using dicing machine (ADT 7100 series) and the diced chips were packaged in different packages (TO- 8, TO-39, QFP, DIP) chosen as per their size and sensing requirement. The device pads were bonded to the package pins using 1 mil aluminium wire.

VI. RESULTS AND DISCUSSION

SAW device contains large number of features to a long distance hence these devices are more prone to defects during fabrication.

These problems can be caused by drift in tool parameters, material problems, or environmental factors. Problems can be the result of an unplanned change in a process parameter or the interaction of two or more process parameters. Examples of each parameter type and its potential impact on lithography process parameters are shown in Table 2.

Table 2: Parameter impacting lithography process

Parameter Type	Source of Variation	Process Parameters Impacted
Tool	Mask Aligner	Focus Alignment Exposure dose Defectivity
Material	Resist	Viscosity Photospeed Defectivity
Material	Developer	Developer concentration Surfactant concentration Defectivity
Material	Water	Defectivity
Material	Wafer	Substrate flatness Substrate reflectivity Substrate topography Defectivity
Environmental	Fab	Temperature Humidity Defectivity

Two key observations can be made from Table II: (1) The lithography process is sensitive to a large number of parameters, some of which are not under the direct control of the lithography process; (2) All parameters have a defectivity component which can directly impact the performance of the lithography process.

As the minimum critical dimensions (CD) required for SAW device fabrication has decreased over time the SAW devices are becoming more sensitive to defect density and maximum defect size. To achieve and maintain yields at economically acceptable levels the SAW device process parameter are optimized in present work for the fabrication of SAW devices.

a. OPTIMIZATION OF PHOTO RESISTS THICKNESS AND UV EXPOSE TIME

Photo resists thickness play a major role in device fabrication [7-9]. For fabrication of sub micron (1.57 µm) feature size, the thickness of the photo resist should be optimised. To achieve the required thickness, photo resists is coated on SAW substrate at different rpm and thickness is measured by ellipsometry system. The photo resist thickness optimisation is shown in figure 5(a).

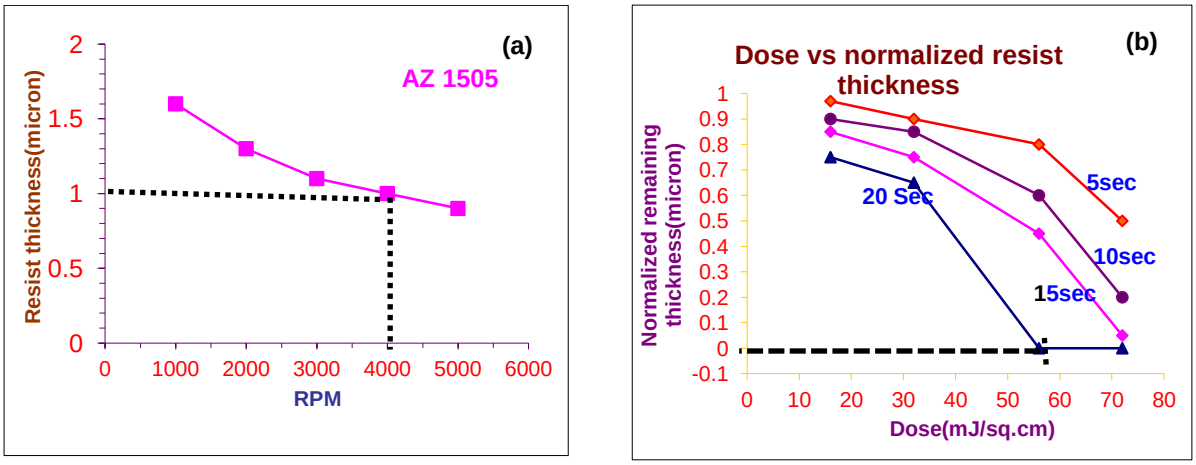

Figure 5. (a) Photo resist thickness optimization (b) Ultra violet energy optimization

After thickness optimisation, UV dose has to be optimized for required feature size, which governs that how much photo resist has remained on the substrate after developing. Figure 5 (b) shows the UV dose and exposing time optimization graph for device fabrication. For the present work the ~ 1 µm thick photo resist film has been used and exposing time 20s has been optimized for ~58 mJ/sq.cm UV energy dose. After optimization, device patterns are printed on the substrate. Substrate is then carefully aligned with the mask pattern and exposed to the optimized ultraviolet light. After exposure, the substrate is then put in a developing solution. Exposed areas undergo a chemical reaction and are removed and we are left with a metal pattern on the device corresponding to the pattern on the mask. The device is then developed and chemically etched so as to remove the metal from the exposed areas.

Since we fabricate number of devices on the same substrate hence the substrate is properly and carefully diced or cut to separate the individual devices. A sophisticated dicing machine accomplishes this process. After successful fabrication, SAW devices are properly packaged in a suitable package as per the requirement.

Figure 6 shows the photograph of the fabricated SAW devices with contact bond pads. Fig. 7(a) shows the SEM images of the mask and fabricated device of 70MHz and 500 MHz SAW

devices. Fig. 7 (b) is the optical microscopic image of the 500 MHZ device showing a closer view of the finger width and gap. As seen from the figures, the finger width and gap between the fingers are equal. The feature sizes are within the range of ±0.1 µm to the expected dimensions and the electrodes have sharp edges indicating acceptable quality of fabrication.

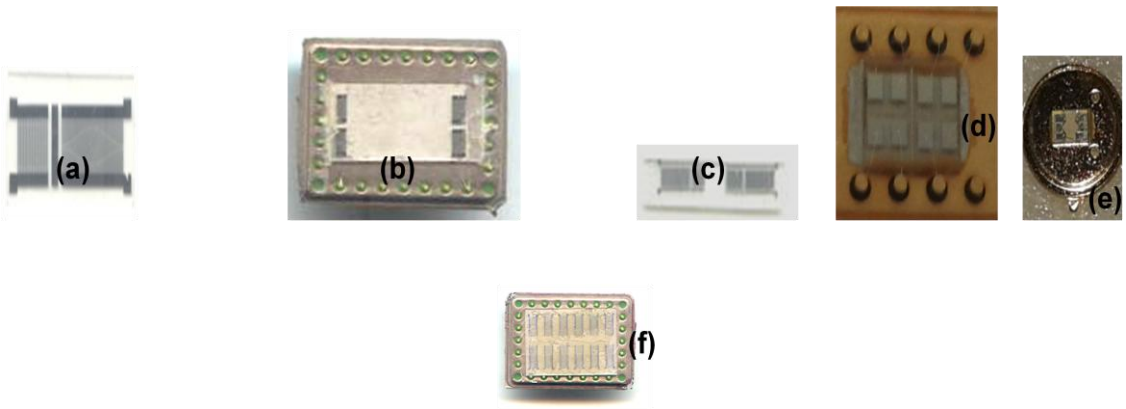

Figure 6. Fabricated devices (a) 70MHz (b)100MHz (c) 150 MHz (d) 273 MHz (e) 500 MHz (f) Multiple Devices

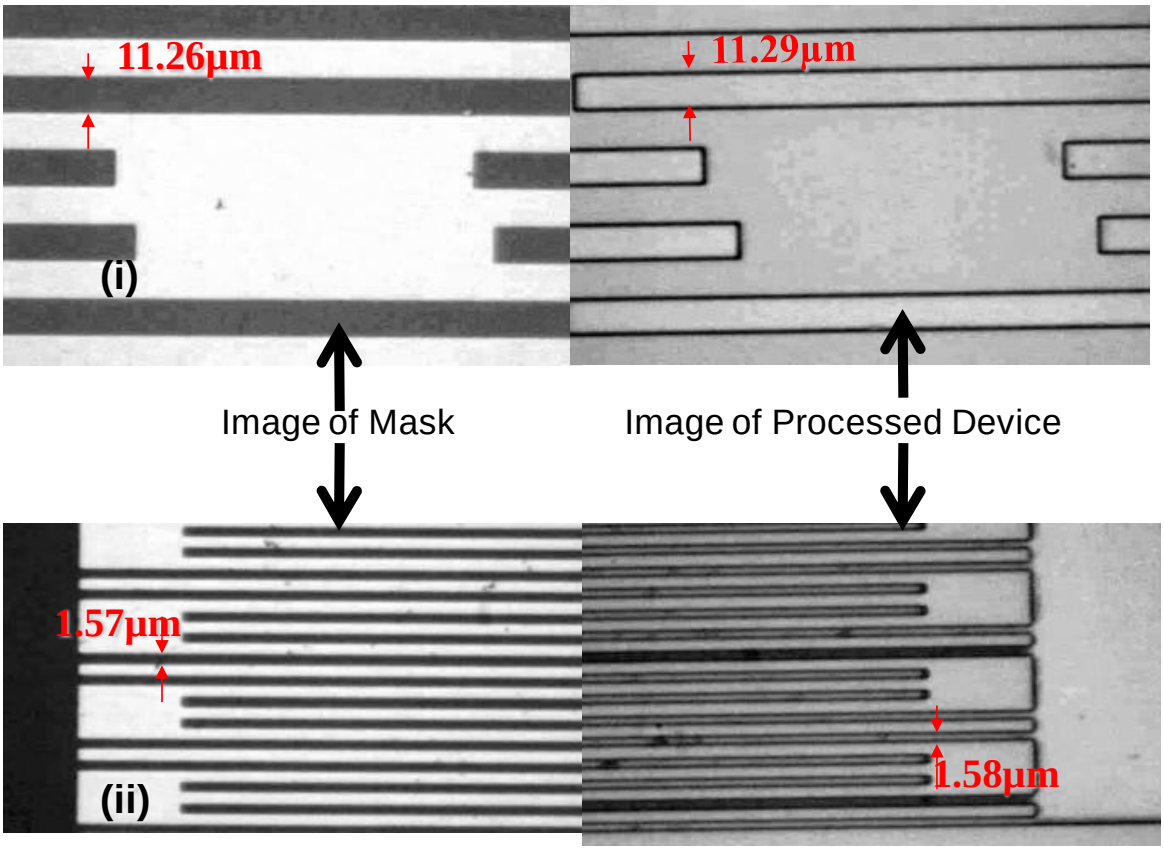

Figure 7 (a). SEM images of Mask and processed device (i) 70 MHz (ii) 500 MHz

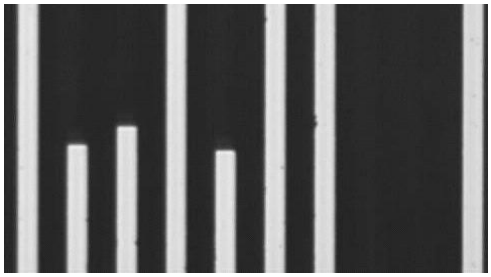

Figure 7 (b). Microscopic images of 500 MHz SAW device.

b. CHARACTERIZATION OF SAW DEVICE

Characterization or testing of device is necessary to validate its design, technology and fabrication. The characterization can either be done in time domain or frequency domain. The time and frequency domains, which are related to each other, are the most common ways of viewing and analyzing any signal of interest. A frequency domain representation includes information on the phase shift that must be applied to each sinusoid in order to be able to recombine the frequency components to recover the original time signal. Frequency domain is a term used to describe the analysis of mathematical functions or signals with respect to frequency. For present work SAW devices are characterized in frequency domain using vector network analyzer (Model ZVR of R&S (Germany) and Model MS4642A of Anritsu (USA)) for their parameter extraction. As we have to use the device in frequency selective component, it is necessary to use the device in oscillator configuration as insertion loss of the SAW device play a major role in oscillator design. Figure 8 shows transmission measurement (S_{21}) of different SAW devices. Table 3 shows the characterization details of the different devices.

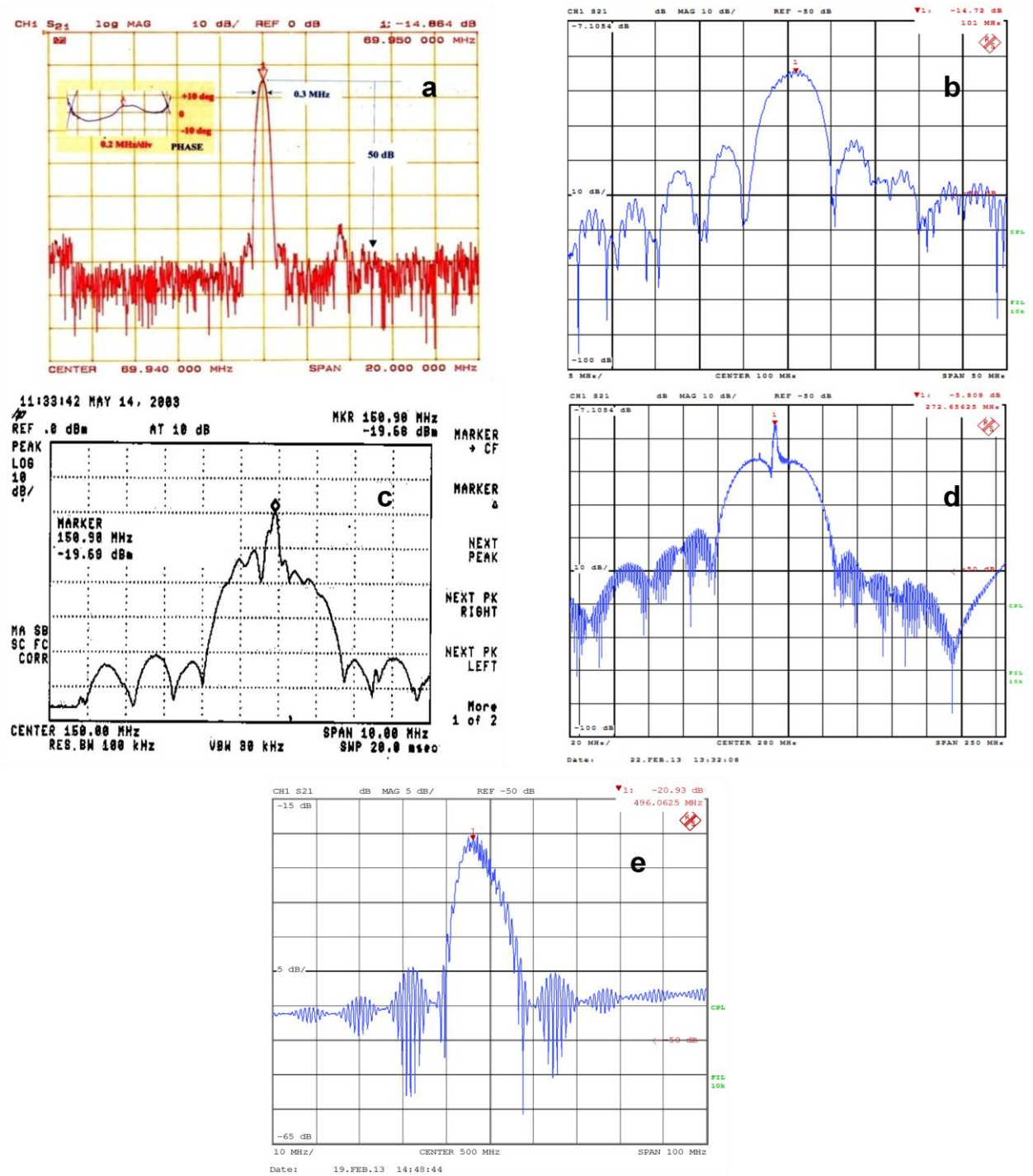

Figure 8. Frequency response of devices (a) 70MHz (b) 100MHz (c) 150 MHz (d)273 MHz

(e) 500 MHz

Table 3: Measured parameters of fabricated SAW devices

S. No.	Centre Frequency (MHz)	Insertion Loss (dB)
a.	**69.9**	**-14.8**
b.	**101**	**-14.72**
c.	**150.90**	**-19.68**
d.	**272.6562**	**-5.808**
e.	**496.025**	**-20.93**

It can be seen in Fig 8 that the minimum insertion loss for device 1 occurs at a frequency of 69.9 MHz and the insertion loss at this frequency is approximately -14.8 dB, for device 2 occurs at a frequency of 101 MHz and the insertion loss at this frequency is approximately -14.72 dB, for device 3 occurs at a frequency of 150.9 MHz and the insertion loss at this frequency is approximately -19.68 dB, for device 4 occurs at a frequency of 272.6562 MHz and the insertion loss at this frequency is approximately --5.808 dB and device 5 occurs at a frequency of 496.025MHz and the insertion loss at this frequency is approximately -20.9 dB. Thus, the resonance frequency of the fabricated SAW devices reasonably matches the theoretically calculated resonance frequency values of the devices with acceptable impedance matching. The accuracy of frequency response characteristics of the fabricated SAW devices validates the high quality of fabrication achieved through the optimized set of fabrication parameters discussed in Section 5.1. The slight variations in the resonance frequencies might have been caused due to slight variation (designed and fabricated) in the finger width and gap of the device as shown in Fig 7 (a) and (b).

c. SENSOR PREPARATION AND CHARACTERIZATION

For single sensor, 150 MHz SAW device and multi sensor array, 500 MHz SAW devices are used. For single and multi sensor application the devices are cut in dual and penta configuration. For sensing the toxic chemicals, SAW device is coated with a selective polymer interface. Before depositing the interface coating, the device is given oxygen plasma treatment for 30s to ensure proper adhesion of polymer film on the device surface. Out of two devices (single sensor) one device is coated with Bisphenol polymer by drop dry method using methanol as a solvent in a clean room environment at room temperature (25^{o}C). For multisensory array, four polymers (PEM-BIS, PEM-HFBP, PPM-BIS, PPM-HFBP) were

coated on the four SAW devices. The amount of material loaded is about 50 ng on the signal path between the transmitting and receiving IDTs. The devices were then baked at 90°C for about 5 hours in nitrogen flow to evaporate any remaining solvent. The devices along with the package were then fitted to a sensor cell for testing in presence of toxic vapours (Nimal et al 2006, Bhasker 2013) [37-39]. The devices were placed in the feedback loop of a two stage amplifier in order to be realized as sensor oscillators. The outputs of the two oscillators, the reference and the sensor were mixed using a double balanced IC mixer and filtered by a passive low pass filter. The output is in kHz frequency which is amplified and passed to digital section for frequency measurement [37]. The sensor system is tested with the very low concentration of DMMP vapor using vapor generator system for sensor characterization (Singh et al 2014) [35]. Nitrogen is used as carrier gas [28-34] and the vapor is generated by flowing nitrogen through a flask placed with a permeation vial containing DMMP (Di-Methyl Methyl Phosponate, a simulant of chemical warfare agent sarin). The sensor is exposed alternately to carrier gas and a mixture of carrier gas and DMMP vapors. The concentration of DMMP is calculated on the basis of weight loss method and same has been cross verified by flam photometric detector (Model AP4C) made by PRONGIN, France. SAW device works as a mass sensor, when analytes of interest (DMMP) comes in contact of the sensor which has been coated with a selective polymer film, than due to adsorption of chemical analytes (DMMP molecules) on the device, the frequency of the oscillator is changed [5,27-30, 33-39]. The change in frequency is then recorded in the PC through data acquisition system. Initially the sensor was refreshed by passing Nitrogen (N_2) gas and then exposed to a certain concentration of DMMP. The transient response curve for several cycles at fixed concentration of 360 ppb for single sensor device at 150 MHZ is shown in figure 9 (a), during refreshing, the device is returned to its original frequency. The response time of the sensor is 15s and recovery time is 45s. There is almost 40 Hz frequency shift is recorded for change in vapour concentration of 360 ppb. When multisensory system is exposed to same concentration (360ppb) of DMMP then almost 1400 Hz frequency shift is recorded for the change in vapour concentration of 360 ppb. It is observed that when we increase the frequency by almost 3.5 times, the sensitivity of the sensor system increases by almost 16 times. Hence by increasing the operating frequency of the sensor we can increase the sensitivity. Results show that there is significant change in frequency due to very small change in DMMP concentration. The output of the device is also highly reproducible. Thus the device has the potential for detecting chemical warfare agents at very low concentration in ppb range.

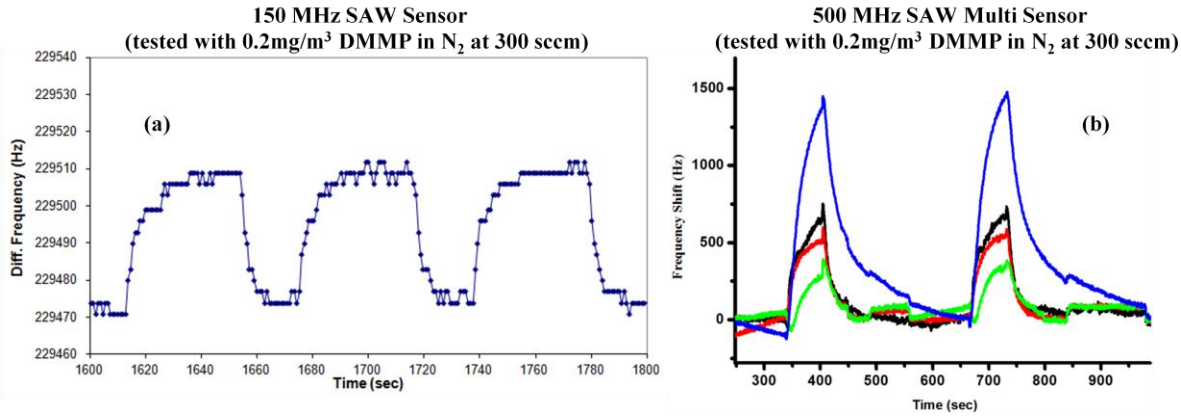

Figure 9. Sensor Testing (a) Single sensor testing with 360 ppb of DMMP (b) Multisensory testing with 360 ppb of DMMP.

VII. CONCLUSION

In the reported work, SAW devices at different frequency were designed and simulated for the optimum parameters such as velocity, coupling coefficient, IDT width and gap, aperture and number of electrode pairs. The designed devices at 70, 100, 150, 273 and 500 MHz are fabricated successfully by conventional optical lithography technique with more accuracy. The frequency response of the fabricated SAW device show excellent match with the simulated response. The SAW devices have been diced in pair for single sensor and in group of five for multisensory sensor array application for the proper cancellation of spurious for realizing reliable SAW chemical sensor. The devices have been coated with selective polymer for selectively detection of toxic chemical vapours. Sensors have been tested with DMMP vapors at very low concentration in ppb range. This sensor shows good sensitivity with significant amount of frequency shift with CW simulent. Sensor shows fast response and recovery times and it also shows good base line stability as it return to it base frequency after purging with N_2 gas. It is demonstrated that, increasing the operating frequency of SAW device, the sensitivity of the SAW based chemical sensor can be enhanced and sensor system can be made for detection of toxic chemical in ppb range using high frequency SAW device.

ACKNOWLEDGEMENT

The authors are thankful to Director, SSPL Delhi and Department of Electrical Engineering, Jamia Milia Islamia University, Delhi, for providing support to carry out the research work. The authors gratefully acknowledge the help and cooperation from their colleagues.

REFERENCES

[1]Ballato, "Piezoelectricity: History and new thrusts," in Proc. Ultrason. Symp., vol. 1, 1996, pp. 575–583.

[2]D. Morgan, "Surface-Wave Devices for Signal Processing", Amsterdam, The Netherlands, Elsevier, 1991, pp. 152.

[3]H. Wohltjen, D. Ballantine, R. White, S. Martin, A. Ricco, E. Zellers, and G. Frye, "Acoustic Wave Sensors Theory, Design, and Physico-Chemical Applications", New York: Academic press, 1997.

[4] J.W. Gardner, V.K. Varadan, O.O. Awadelkarim, "Microsensors, MEMS, and Smart Devices", John Wiley & Sons Ltd, Chichester, 2001.

[5] D. Matatagui, M. J. Fernandez and J. Forntecha, "Love-wave sensor array to detect, discriminate and classify chemical warfare agent simulants", Sens. Actuators B Chem., vol.175, **2012**, pp. 173–178.

[6] K. Uehara, C. M. Yang, T. Shibata, S.-K. Kim, S. Kameda, H. Nakase, et al. "Fabrication of 5-GHz-band SAW filter with atomically-flat-surface AlN on sapphire", IEEE Ultrasonics Symposium, 2004, pp. 203–206.

[7] J.M. Kontio, J. Simonen, J. Tommila, M. Pessa, "Arrays of metallic nanocones fabricated by UV-nanoimprint lithography", Microelectron. Eng. vol. 87, 2010, pp. 1711–1715.

[8] F. D. Lai and H. M. Huang, "Fabrication of High Frequency and Low-Cost Surface-Acoustic Wave Filters Using Near Field Phase Shift Photolithography," Microelectronic Engineering, Vol. 83, No. 4, 2006, pp. 1407-1409.

[9] E. Forsén, D. Nilsson, S. Ballandras, E. Mayer, S. Sakharov, "Jet-and-Flash Nano Imprint Lithography: Fabrication of Passive Wireless Surface Acoustic Wave Sensors", Proceeding Eurosensors XXV, 2011, pp. 860–863.

[10] J.J.K. Kim, S. Paik, F. Herrault, M.G. Allen, "UV-LED lithography for 3-D high aspect ratio microstructure patterning", 14th Solid State Sensors, Actuators, and Microsystems, Workshop, 2012, pp. 481–484.

[11] J. Liu, S. He, "Fast calculatation of the paramters of SAW coupling-of-modes model", Chin. J. Acoust. Vol. 26, 2007, pp. 123-127.

[12] L. Fan, H. Ge, S. Zhang, H. Zhang and J. Zhu, "Optimization of sensitivity induced by surface conductivity and sorbed mass in surface acoustic wave gas sensors". Sens. Actuators B, vol. 161, 2012, pp. 114–123.

[13] L. Fan, S. Zhang, H. Ge, and H. Zhang, "Theoretical optimizations of acoustic wave gas sensors with high conductivity sensitivities", Sens. Actuators B, vol. 171–172, 2012, pp. 1272–1276.

[14] M. Schweyer, J. Hilton, J. Munson, and J. Andle, "A novel monolithic piezoelectric sensor," in Proc. Ultrason. Symp., vol. 1, 1997, pp. 371–374.

[15] S. Martin et al., "Gas sensing with acoustic devices," Proc. Ultrason. Symp., vol. 1, 1996, pp. 423–434.

[16] R. Kshetrimayum, R. D. S. Yadava, and R. P. Tandon, "Modeling electrical response of polymer-coated SAW resonators by equivalent circuit representation.," Ultrasonics, vol. 51, no. 5, Jul. 2011, pp. 547–553,

[17] S. Thomas, S. L. T. Leong, Z. Rácz, M. Cole, and J. W. Gardner, "Design and Implementation of a High-Frequency Surface Acoustic Wave Sensor Array for Pheromone Detection in an Insect-inspired Infochemical Communication System," 14th International Meeting on Chemical Sensors, 2012, pp. 11–14,

[18] H. Wohltjen, "Surface acoustic wave microsensors," Proc. 4th Int. Solid-State Sens. Actuators Conf., 1987, pp. 471–477.

[19] J. Grate, S. Martin, and R. White, "Acoustic wave microsensors," Anal. Chem., vol. 65, no. 21, 1993, pp. 940–948.

[20] J.W. Grate, "Hydrogen-bond acidic polymers for chemical vapor sensing". Chem. Rev., vol. 108, 2008, pp. 726-745.

[21] C.Wold et al., "Temperature measurement using surface skimming bulk waves," Proc. Ultrason. Symp., vol. 1, 1999, pp. 441–444.

[22] D. Cullen and T. Reeder, "Measurement of SAW velocity versus strain for YX and ST quartz," in Proc. Ultrason. Symp., 1975, pp. 519–522.

[23] D. Cullen and T. Montress, "Progress in the development of SAW resonator pressure ransducers," in Proc. Ultrason. Symp., vol. 2, 1980, pp. 519–522.

[24] A. Pohl, G. Ostermayer, L. Reindl, and F. Seifert, "Monitoring the tire pressure at cars using passive SAW sensors," Proc. Ultason. Symp., vol. 1, 1997, pp. 471–474.

[25] A. Lonsdale, "Method and apparatus for measuring strain," U.S. Patent 585 571, Dec. 17, 1996.

[26] W. Bowers, R. Chuan, and T. Duong, "A 200 MHz surface acoustic wave resonator mass microbalance," Rev. Sci. Instrum., vol. 62, no. 6, 1991, pp. 1624–1629.

[27] V.B. Raj, H. Singh, A.T. Nimal, M.U. Sharma, M. Tomar and V. Gupta, "Origin and role of elasticity in the enhanced DMMP detection by ZnO/SAW sensor" Sensors and Actuators B:Chemical, vol. 207, 2015, pp.375-382

[28] K.Vetelino, P. Story, R. Mileham, and D. Galipeau, "Improved dewpoint measurements based on a SAW sensor," Sens. Actuators B, Chem., vol. 35-36, 1996, pp. 91–98.

[29] J. Cheeke, N. Tashtoush, and N. Eddy, "Surface acoustic wave humidity sensor based on the changes in the viscoelastic properties of a polymer film," Proc. Ultrason. Symp., vol. 1, 1996, pp. 449–452.

[30] E. Radeva and I. Avramov, "Humidity sensing properties of plasma polymer coated surface transverse wave resonators," in Proc. Ultrason. Symp., vol. 1, 1998, pp. 509–512.

[31] L. Reindl, C. Ruppel, A. Kirmayr, N. Stockhausen, and M. Hilhorst, "Passive radio requestable SAW water content sensor," Proc. Ultrason. Symp., vol. 1, 1999, pp. 461–466.

[32] M. Vellekoop and B. Jakoby, "A love-wave ice detector," Proc. Ultrason. Symp., vol. 1, 1999, pp. 453–456.

[33] H. Wohltjen and R. Dessy, "Surface acoustic wave probe for chemical analysis I: Introduction and instrument design," Anal. Chem., vol. 51, no. 9, 1979, pp. 1458–1475.

[34] E. Staples, "Electronic nose simulation of olfactory response containing 500 orthogonal sensors in 10 seconds," Proc. Ultrason. Symp., vol. 1, 1999, pp. 417–423.

[35] H. Singh, V. B. Raj, J. Kumar, U. Mittal, M. Mishra, A.T. Nimal, M.U. Sharma, and V. Gupta, "Metal oxide SAW E-nose employing PCA and ANN for the identification of binary mixture of DMMP and methanol", Sensors and Actuators B, vol. 2004, 2014, pp. 147-156.

[36] Asif I. Zia, S. C. Mukhopadhyay, Pak-Lam Yu, I.H. Al-Bahadly, Chinthaka P. Gooneratne, Jürgen Kosel, "Rapid and Molecular selective electrochemical sensing of phthalates in aqueous solution" Biosensors and Bioelectronics, 67:342-349 15 May 2015

[37] A.T. Nimal, M. Singh, U. Mittal, and R.D.S. Yadava, "A comparative analysis of one port colpitt and two port pierce oscillators for DMMP vapour sensing", Sensors and Actuators B, vol. 114, 2006, pp. 316-325.

[38] V.B. Raj, H. Singh, A.T. Nimal, M.U. Sharma, and V. Gupta, "Oxide thin films (ZnO, TeO2, SnO2, and TiO2) based surface acoustic wave (SAW) E-nose for the detection of chemical warfare agents", Sensors and Actuators B, vol. 178, 2013, pp.636-647.

[39] V.B. Raj, A.T. Nimal, Y. Parmar, M.U. Sharma, K. Sreenivas and V. Gupta, "Cross-sensitivity and selectivity studies on ZnO surface acoustic wave ammonia sensor", Sensors and Actuators B, vol. 147, 2010, pp. 517–524.